International Journal of Progressive Sciences and Technologies (IJPSAT)
ISSN: 2509-0119.

http://ijpsat.ijsht-journals.org
Vol. 28 No. 2 September 2021, pp.572-583

A Quantum Mechanical Viewpoint on Structural Stability of the Smallest Hydrated Sulfate Cluster $[SO_4(H_2O)_3]^{2-}$

Anant Babu Marahatta[1, 2]

[1]Department of Chemistry, Amrit Science Campus, Tribhuvan University, Kathmandu, Nepal
[2]Engineering Chemistry Unit, Kathford International College of Engineering and Management (Affiliated to Tribhuvan University), Kathmandu, Nepal

Abstract – Being the most kosmotropic type anion, SO_4^{2-} shows a very strong affinity towards sequential hydration, and hence undergoes immediate stabilization *via* differently sized hydrated clusters $[SO_4(H_2O)_n]^{2-}$, $n \leq 80$ in solution state. Interestingly, the smallest yet stable hydrated cluster detected through the advanced experimental techniques is $[SO_4(H_2O)_3]^{2-}$ with hydration number $n = 3$. Despite its ubiquity in many sulfate enriched aqueous systems, the concerned electronic structure and structural stability reported so far are mostly based on the position of atomic nuclei in the theoretically produced low energy molecular geometry, which is, however, not regarded as a quantitative approach for depicting chemical bonding and structural entity in respect to electron density distributions around atoms and bonds between the atoms. In this study, the molecular orbitals (MOs) and Mulliken population analysis methods are used to extract chemical bond related information of $[SO_4(H_2O)_3]^{2-}$ from its DFT derived molecular wavefunctions (Ψ) and then total molecular electron density surface (TMEDS), MOs iso-surfaces, and contour lines are deeply analyzed prior to describe how these EDSs actually provide detailed insights into the orbital interactions, atomic bonding, and structural stability. It is found that $[SO_4(H_2O)_3]^{2-}$ ion stabilizes with (a) a closed 3D structural entity and a realistic distribution of electron cloud around the specific atoms and bonds, (b) a delocalized type electron density, and (c) an orbital type bonding interaction between the atoms. Besides these, a quantitatively measured electron amplitudes and the specific type bonding interactions make that hydrated structure quantum mechanically feasible.

Keywords – Trihydrated sulfate, Molecular orbitals, Contour maps, and Bonding analysis.

I. INTRODUCTION

The divalent sulfate ion (SO_4^{2-}) is a very important inorganic radical found most abundantly in several sulfate mineral-enriched aqueous systems such as electrolytes of flow battery technology [1], [2]; human body fluids [3]; liquid beverages such as beer, juice, milk, wine, mineral water etc.; foods and vegetables such as almonds, broccoli, bread, cauliflower etc.; laxatives used for medical treatments such as Na_2SO_4 solution [4] as well as in variably sized mixed particles suspensions such as atmospheric aerosols. Biologically, this ion is regarded as one of the most essential micronutrients in human tissues, cells, and plasma (~300 μM), and therefore becomes a principal source for sulfur in many organisms: an optimal supply of the sulfate ions is made through influx and efflux mechanisms occurred in each cell [5]. In pharmaceutical processes, the SO_4^{2-} ions are highly useful in the various stages of protein extraction and purification due to their kosmotropic nature (SO_4^{2-} ion is placed at the most kosmotropic end of the Hofmeister series of anions: $SO_4^{2-} > HPO_4^{2-} > CH_3COO^- > Cl^- > NO_3^-$) [6], [7]. Beyond this, these ions are believed to be the prime scatterers of solar radiation and the prominent participants in cloud formation process [8] [9]. Because of their ubiquitous presence and various significance, they were already recognized with high assurance as a negatively charged chemical unit (one SO_4^{2-} occupies two charged sites) possessing distinct structural features and chemical properties. However, their instability in free and isolated states observed through various experimental tools [10], [11], [12], [13], [14], [15], [16] made scientific community quite suspicious and indecisive at the very initial stage. Subsequently, the explanation revealed through the theoretical computations as "the main cause of sulfate ions inexistence in free-state is due to a strong intramolecular type Coulombic repulsion between the

Corresponding Author: Anant Babu Marahatta

two excess electrons carried by themselves" was found to be more convincible and logical [17].

In the past recent years, the SO_4^{2-} ion has been considered as a charged species having strong affinity towards sequential hydration and getting stabilized through variably sized hydrated clusters in solution and in gaseous states, and counter cations in solid state [18]. Interestingly, how a free and an isolated state of SO_4^{2-} gets hydrated in an aqueous solution and stabilized structurally and energetically is already accounted by the present author and reported the findings elsewhere [14], [15], [16] with thorough consideration of molecular level interactions, step-wise-hydration mechanisms (molecule-by-molecule), and quantitative structure property relationships (QSPR) (size of the hydrated clusters was limited to $[SO_4(H_2O)_n]^{2-}$, n = 1−4 & 16) by employing density functional theory (hereafter, DFT) based quantum mechanical model. However, to the knowledge of this author, the most intriguing fact of sulfate ion hydration "$[SO_4(H_2O)_3]^{2-}$ with hydration number n = 3 is the smallest yet stable hydrated structure of SO_4^{2-}" reported earlier by the series of experimental and theoretical research works [10,] [11], [12], [13], [14], [15], [16], [17], [18] has not captivated much interests of the researchers so far. According to these literatures, significant number of $[SO_4(H_2O)_3]^{2-}$ entities were detected through photodetachment, infrared photodissociation, and gas phase cluster spectroscopies whose ground state electronic structure and energetic stability were studied through DFT:B3LYP, *ab initio*, basin-hopping Monte Carlo, and Coalescence Kick (PBE0/6-31+G*) methods. But, the way the authors have confirmed molecular electronic structures and bonding interactions in $[SO_4(H_2O)_3]^{2-}$ simply by looking into the position of concerned atomic nuclei in the computationally derived low energy molecular geometry is not much recognized as a quantitative quantum mechanical approach in terms of electron density distributions around atoms and bond between the atoms. Therefore, this study is mainly aimed at realizing the structural entity of this microhydrated cluster more practically and depicting the precise quantitative picture of its chemical bonding and structural stability through the molecular wavefunctions based quantum mechanical methods.

It is very apparent to the theoretical/computational chemists that a precise quantitative interpretation of bonding interactions between the atoms in their structural entity can only be done by looking seriously into the quantum mechanically derived electron density: a direct quantitative picture for the molecular wavefunctions Ψ. Since the Ψ is invisible directly, but can be expressed mathematically as a sum of the products of individual molecular orbitals Ψ_i containing spin paired electrons, one should always look at the total molecular electron density (a squared of the $\Psi(\Psi^2)$) surface, individual MOs' iso-surfaces and contour linings [19], [20], [21]. In quantum mechanics, this type of quantitative bonding inspection method is known as MOs analysis because MOs are the solutions to the Schrodinger wave mechanical equation, wavefunctions Ψ, and electrons' most-probable sites [22]. Strictly speaking, the MOs (expanded in terms of Slater-type atomic orbitals (STOs) or Gaussian-type atomic orbitals (GTOs)) are electron rich mathematical functions that can only be used to depict electronic location and electronic wave like behavior in the molecular specimens [23]. So, in order to reveal how electronic charges associated with MOs, AOs, and atomic centers are disseminated throughout the molecular specimens, population analysis methods [19] must be used. While these methods are mainly based on how electron density is actually partitioned, a Mulliken method where some arbitrary and orbital based scheme is used to partition molecular wave function is widely employed computational mean in examining electronic charges redistribution and bond populations in the bulk materials due to its post-processing type computational procedure [24], [25]. As a whole, the Mulliken derived atomic charges are used to approximate charge distribution throughout the $[SO_4(H_2O)_3]^{2-}$ specimen plus to quantify & compare specific type bonding interactions, and the total molecular electron density surfaces, MOs iso-surfaces & their contours are used to explain structural entity, stability, and bonding electronic interactions of this microhydrated cluster quantitatively.

Computationally, both MOs and Mulliken based methods are routinely carried out through those quantum mechanical models that are developed on the basis of LCAO MO (Linear combination of the atomic orbitals molecular orbitals) approximations [24], [25]. The DFT model is one of them as it is based on LCAO-Kohn-Sham ansatz [26], [27] with unique functional of electron density, and is widely recognized as an efficient scheme to compute electronic structures/ energies and MOs of many-body-systems [28], [29], [30], [31]. In this contribution, the DFT model with hybrid B3LYP functionals is applied to $[SO_4(H_2O)_3]^{2-}$ cluster, and investigated its structural stability and bonding interactions in the light of wavefunction based MOs and Mulliken methods. Basically, the DFT derived total molecular electron density surfaces, MOs iso-surfaces, contour diagrams, and Mulliken partial atomic charges of the $[SO_4(H_2O)_3]^{2-}$ ion are used to access its electron density distributions around atoms and bonds between the atoms, and to underscore how these electron density surfaces actually provide meaningful explanation to orbital interactions, atomic bonding, and specific electronic interactions quantitatively. The structure of this paper is organized as follows: the computational details are outlined in section 2, the results and discussions are presented in section 3, and the conclusions are summarized in section 4.

II. Computational Details

Prior to compute 3D total electron density surfaces, MOs iso-surfaces & their contour maps of $[SO_4(H_2O)_3]^{2-}$ cluster, and the Mulliken partial atomic charges of each atom, the most stable electronic structure of it was determined theoretically by using computationally designed molecular model as its trial structure. It was carefully built in *GaussView*: the Gaussian graphical interface [32], and the set of Cartesian coordinates for each atom was extracted before starting energy minimization (geometry optimization) calculations. The specific *Gaussian* keywords and methodologies were selected as instructed in *Gaussian* 09 manual [33]. The hybrid functional based DFT method known as B3LYP was employed with the basis set of this type: 6−31G (*d*, *p*) *i.e.*, the methodology applied was DFT: B3LYP/6−31G (*d*, *p*). To route the *Gaussian* scheme for carrying out desirable computations, ionic charge and spin multiplicity were specified as two integers in the format of (charge, spin multiplicity). Since $[SO_4(H_2O)_3]^{2-}$ is an anionic specimen carrying two units of negative charge, the set of integers used was (−2, 1). While solving Schrodinger equation iteratively, the self-consistent field (hereafter, SCF) with both default SCF procedure (SCF=Tight) and Berny algorithm for geometry optimizations to a local minimum were selected in *Gaussian* 09 [33], [34]. As current interest of this author lies in the study of structural and bonding stability of $[SO_4(H_2O)_3]^{2-}$ through two wavefunction based methods *viz*; (a) MOs analysis: all the required 3D total electron density surfaces and MOs iso-surfaces with their contours were produced separately, and (b) Mulliken population analysis: all the Mulliken derived partial atomic charges were displayed in the DFT optimized ground state electronic structure on the basis of color indices and ranges plus respective numeral atomic charges were extracted, each of these two *Gaussian* output files (such as *.log*, and *.fchk*) containing three dimensionally displayed chemical data were carefully analyzed through *GaussView*, and sketched all the density surfaces/contours in the 3D plot axis at a standard set of |isovalue|: MO = 0.0200, Density = 0.0004 (Figure 1 and Figure 2).

III. Results and Discussions

3.1. Chemical Bond Analysis

In chemistry, a chemical bond is simply defined as the force that binds atoms together in a chemical compound. This force actually arises as a result of electronic distribution between the two nearby atoms that interact each other through valence electrons. This is why, the theoretical chemists/physicists always give keen interest in chemical bonds for the sake of acquiring semiquantitative type bonding and structural information which in turn are applicable to confirm geometrical stability of the molecular/ionic compounds in terms of wavefunction based parameters. While two electronic theories of chemical bond namely Lewis and VSEPR consider bonding and lone pair electrons as their central key-point for predicting molecular geometry and structural orientation, the quantum mechanical theory (hereafter, QMT) critically describes electronic distributions in atoms through the wave functions and eagerly explains the role of bonding electrons in terms of orbitals (orbital concept) thinking about the electronic probabilistic matter waves [36], [37]. Therefore, the QMT is more popular among the researchers more especially for the extensive evaluation of wave like behavior of bonding and non-bonding electrons distributed throughout the molecular specimen which eventually provides a precise theoretical mean for depicting quantitative picture of the chemical bonding and molecular geometry.

In order to account the wave nature of electrons inside each atom, the QMT implements Schrödinger wave mechanical equation that has an ability to describe energy and position of the electrons in space and time. More specifically, a complete solution of the Schrödinger equation describes electronic wavefunction Ψ and its squared Ψ^2 which guides us in determining orientation and shape of the molecular orbitals where electrons find maximum probability to reside inside the molecular system. Such information could be useful to provide better quantum mechanical insights into the electronic interactions and electronic distributions in chemical bonding [38], [39]. But, due to immeasurable and rigidly undefined concept of the bonding electronic interactions, it is not easy to extract all the chemical bond related information from the molecular wavefunction Ψ [40]. However, a number of ways that fall into these four groups: (a) Molecular orbital analysis, (b) Population analysis, (c) Electron density analysis, and (d) Energy analysis, are available for directly analyzing the concerned solution of the Schrödinger equation as well as quantifying electronic plus bonding interactions quantum mechanically. Even though none of them are capable enough to fully capture principal characteristic features of the chemical bonds due to complex and not rigorous type electronic interactions, they are recognized as indispensable theoretical tools while extracting wave mechanical information of the chemical bonds from the concerned molecular wavefunction Ψ [38], [39], [40]. In this contribution, the first two methods, *viz*. Molecular orbital, and Population analysis are used to analyze the DFT based theoretical calculations of trihydrated sulfate ion $[SO_4(H_2O)_3]^{2-}$ on the basis of which the structural stability, bonding and electronic interactions in it are investigated quantum mechanically. The corresponding

results are summarized below in the subsections 3.1.1 and 3.1.2 respectively.

3.1.1 Molecular Orbitals (MOs) Analysis

In quantum mechanics, an LCAO approach of the MO theory is based on the fact that an equivalent number of new MOs (Ψ) are formed whenever the concerned atomic orbitals (Ψ_i) of the bonding atoms are mixed up [41]. This wave mechanical perspective is utilized while constructing MO energy level diagrams for multi-atomic molecular systems that are, however, just useful to describe qualitative aspects of the chemical bonding rather than giving its realistic views. Fortunately, all the MOs that are involved in making MO diagrams can be computed quantum mechanically in the form of single total molecular electron density surface and in their separate single sets. Figure 1 and Figure 2 display the DFT derived 3D total molecular electron density surface for $[SO_4(H_2O)_3]^2$ and its individual MOs iso-surfaces with their contours respectively. The 3D density surface shown in Figure 1(b) was actually generated through the complete association of the electron density of all the individual MOs including those listing in Figure 2. In fact, this total electron density surface represents three dimensional electron density distributions around the specific nuclei of $[SO_4(H_2O)_3]^{2-}$ along with depicting probability of finding electrons around them in the 3D space. The same is the reason why this three dimensional electron density surface is used while approximating a molecular geometrical pattern and a closed 3D molecular geometry with symmetric/asymmetric electronic distributions around the specific atoms. Similarly, while referring to the total electron density surface of $[SO_4(H_2O)_3]^{2-}$, the clearly distinguishable protrusions (electron dense regions) appeared on it can speculate the orientations of centrally located SO_4^{2-} inbound to three H_2O molecules in the 3D axis, giving a stable rigid type hydrogen bonded structural unit. Just for reference, the DFT derived ground state electronic structure of $[SO_4(H_2O)_3]^{2-}$ and it's structural parameters measured in the positions of concerned atomic nuclei are shown in Figure 1(a) whose shape looks as consistent as that approximated by the 3D total molecular electron density surface.

Despite exact sketching of the 3D distribution of electrons around the concerned atomic nuclei in $[SO_4(H_2O)_3]^{2-}$, the total electron density surface is unable to give insights into the specific arrangement of electron density in the particular type bond formation process. Therefore, the 3D electron density iso-surfaces for each individual MOs of $[SO_4(H_2O)_3]^{2-}$ are extracted separately, and observed closely through which the atom-centered, localized/delocalized sites of the electron density, and the maximum probability of finding electron clouds in the atomic proximity are traced out. This sort of information has provided us a quantitative picture for elucidating each chemical bonding and every electronic interactions in $[SO_4(H_2O)_3]^{2-}$. In the support of the same, the contour lines for each individual MOs are constructed simply by taking a slice through this hydrated structure along a plane joining the specific atoms. **Figure 2** shows the electron density surfaces and contour lines for each set of the real bonding MOs (containing two electrons with opposite spin) of $[SO_4(H_2O)_3]^{2-}$ (core MOs **1a-12a** which show significantly less electronic distributions around the specific bond are selectively excluded, as well as nonbonding MOs). The caption includes DFT derived Eigen value (E) for each MO in atomic unit (*a. u.*; Hartree E_h), and the general iso-surface value used for generating MO's density surfaces. Unfortunately, the atomic orbitals mixing coefficients (required for constructing MOs through LCAO approach) are not computed here as this study is mainly aimed at explaining structural stability of $[SO_4(H_2O)_3]^{2-}$ through molecular orbital methods rather than carrying out natural bond order (NBO) analysis. The careful analyses of electron density surface and the particular contour region of each individual MO reflect that the electron density in $[SO_4(H_2O)_3]^{2-}$ remains delocalized over its entire region (the symmetry property of the MO). Again, such delocalized type electron density surface of each individual MOs (Figure 2) unanimously describes uniform/non-uniform electronic distribution over the entire region of $[SO_4(H_2O)_3]^{2-}$ along with approximating a particular region of space in which valence electrons are likely to be found (spatial distribution of the electrons). Similarly, a critical analysis of each electron density surface (Figure 2) made us to assure that all the MOs are originated as a result of the orbital interactions between two or more than two atomic orbitals. As a whole, all these quantum mechanical interpretations for $[SO_4(H_2O)_3]^{2-}$ ion have set out it's complete picture of the 3D molecular structure in which electrons are not localized to the individual bond exist in between two dissimilar atoms, but remain as a cloud delocalized over the entire molecular specimen. For the further clarifications, the contour lines of each contour map (of each MO) extended over $[SO_4(H_2O)_3]^{2-}$ (Figure 2) are used as they show electron amplitudes that measure maximum departure of the electronic wave from its average value. In conclusion, the DFT derived contour maps and the electron density surface plots of each individual Mos semiquantitatively confirm electronic interactions and chemical bonding with structural stability and molecular entity of this microhydrated sulfate ion quantum mechanically. These electronic delocalization phenomena and the quantum mechanical aspects of structural interpretations, however, were not obvious through valence bond theory (VBT) which principally uses hybrid orbitals assigned to specific atoms and assumes chemical bonds as the

localized pairs of bonding electrons.

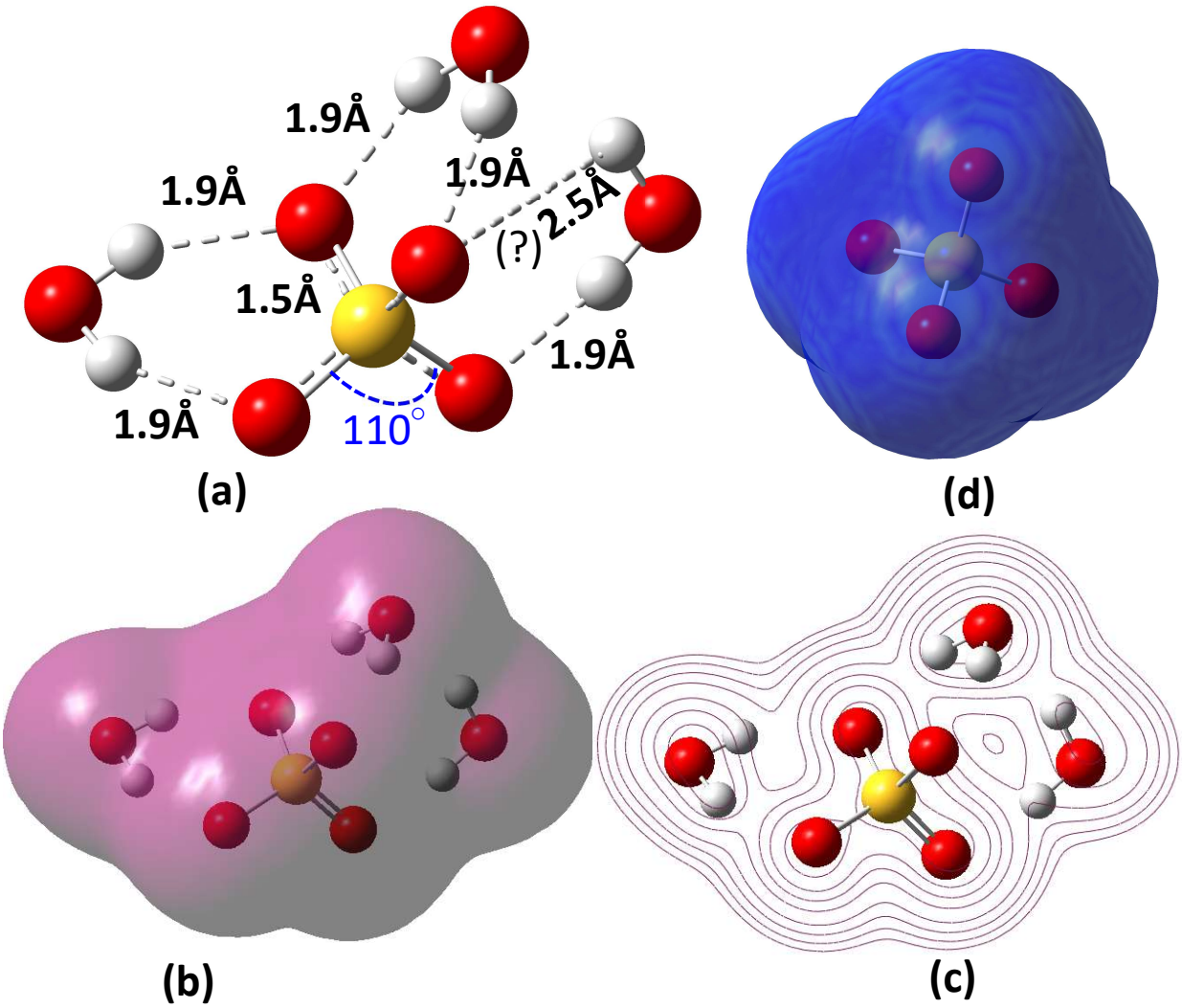

Figure 1. DFT derived (a) ground state electronic structure, (b) total electron density surface (EDS) at an |isovalue|: MO = 0.0200, Density = 0.0004, and (c) contour lines, of $[SO_4(H_2O)_3]^{2-}$ ion. The individual bonding MOs that make up this EDS are shown in Figure 2. Just for reference, the total EDS (transparent mode) for an unhydrated SO_4^{2-} ion is shown in (d).

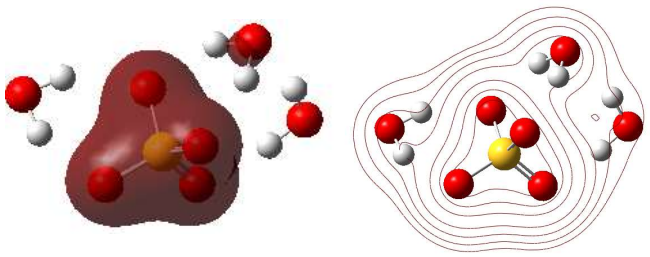

(1) 13a MO and contours, $E = -0.76704$ *a.u.*

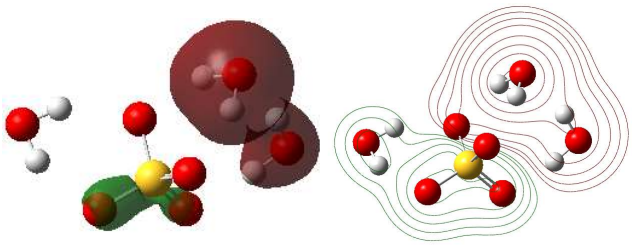

(2) 14a MO and contours, $E = -0.68384$ *a.u.*

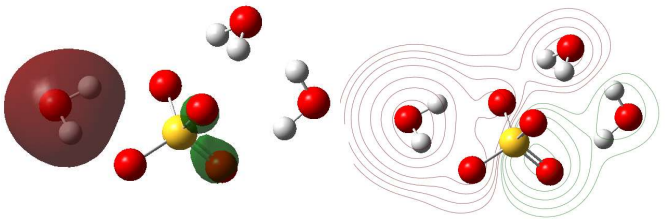

(3) 15a MO and contours, $E = -0.66771$ *a.u.*

(4) 16a MO and contours, $E = -0.66191$ *a.u*

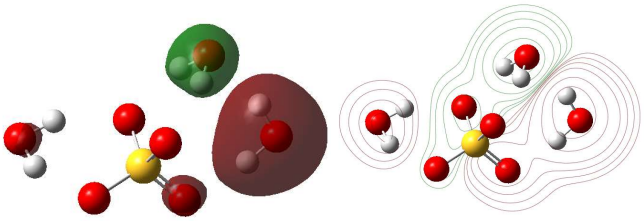

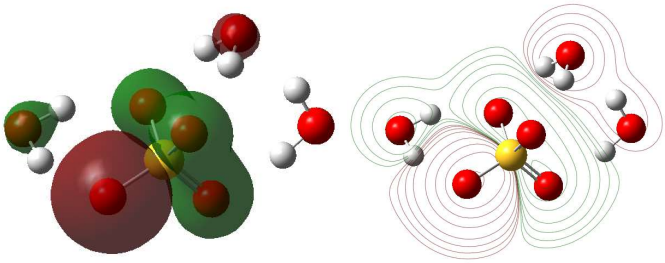

(5) 17a MO and contours, $E = -0.61197$ *a.u*

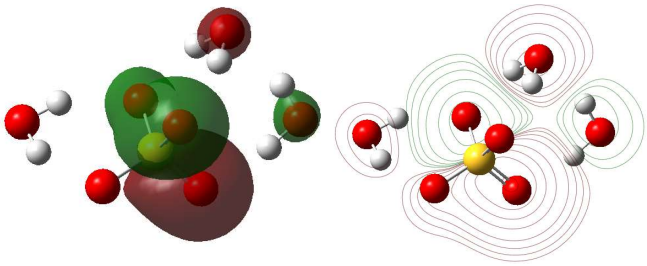

(6) 18a MO and contours, $E = -0.60941$ *a.u.*

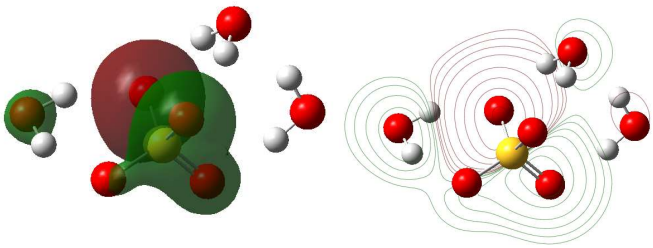

(7) 19a MO and contours, $E = -0.60786$ *a.u.*

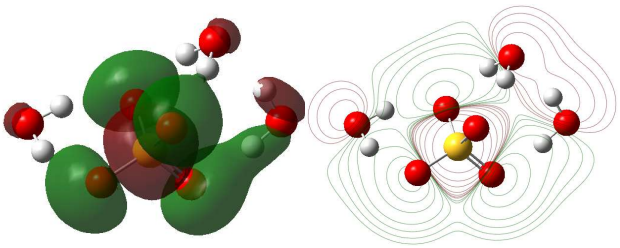

(8) 20a MO and contours, $E = -0.23012$ *a.u.*

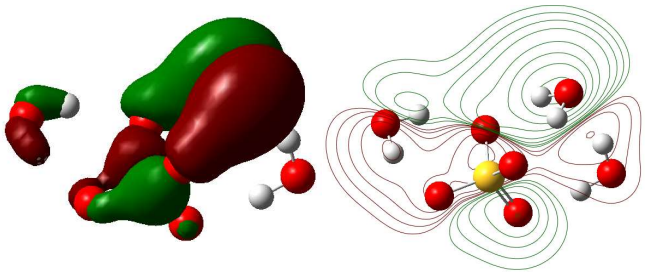

(9) 21a MO and contours, $E = -0.18237$ *a.u.*

(10) 22a MO and contours, $E = -0.17543$ *a.u.*

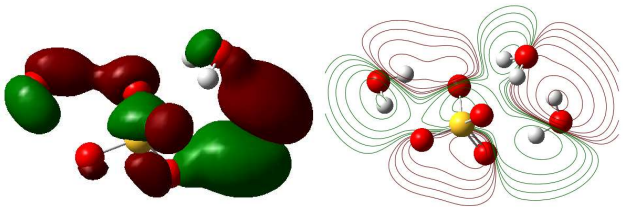

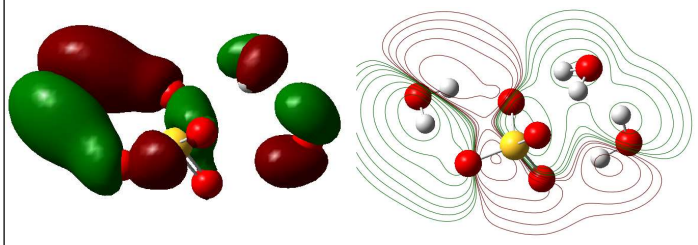

(11) 23a MO and contours, $E = -0.17056$ *a.u.*

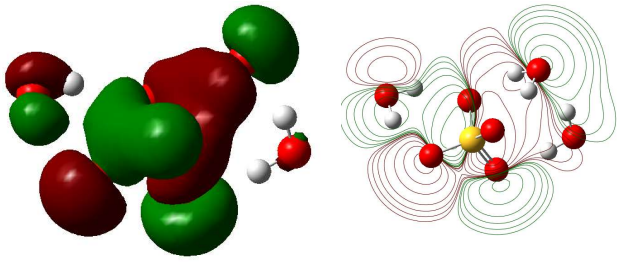

(12) 24a MO and contours, $E = -0.11670$ *a.u.*

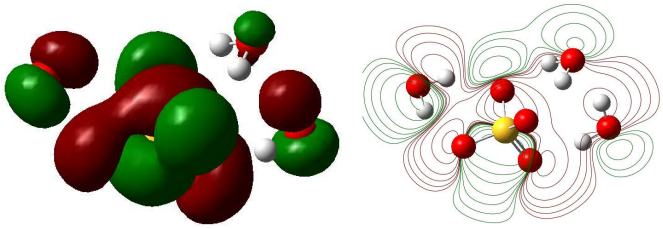

(13) 25a MO and contours, $E = -0.11420$ *a.u.*

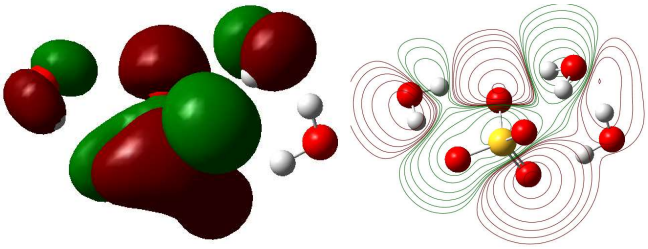

(14) 26a MO and contours, $E = -0.11179$ *a.u.*

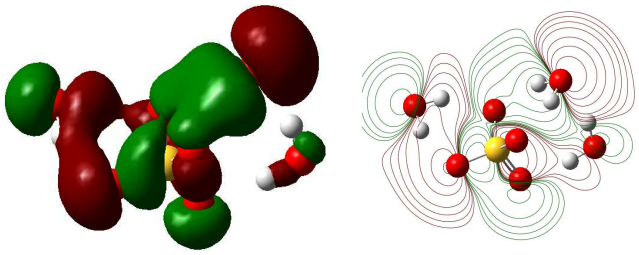

(15) 27a MO and contours, $E = -0.09219$ *a.u.*

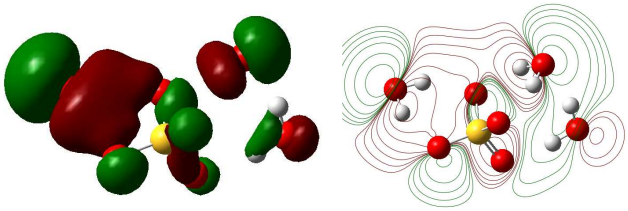

(16) 28a MO and contours, $E = -0.07858$ *a.u.*

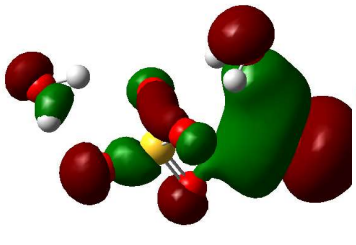

(17) 29a MO and contours, *E* = − 0.06619 *a.u.*

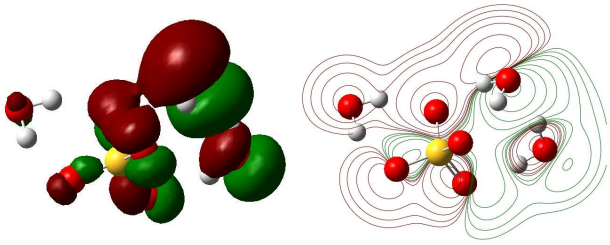

(18) 30a MO and contours, *E* = + 0.00831 *a.u.*

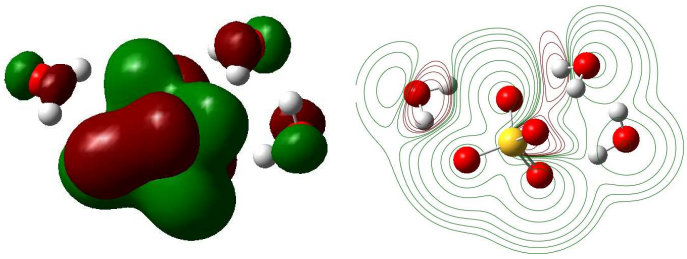

(19) 31a MO and contours, *E* = +0.01221 *a.u.*

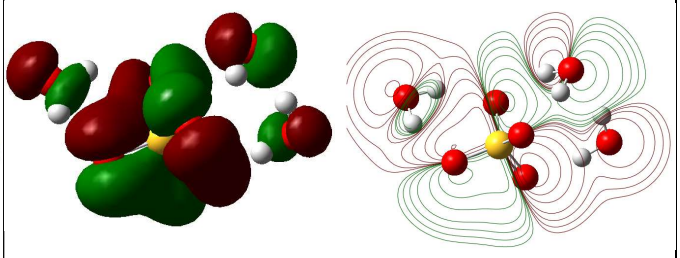

(20) 32a MO and contours, *E* = +0.01427 *a.u.*

(21) 33a MO and contours, *E* = +0.01988 *a.u.*

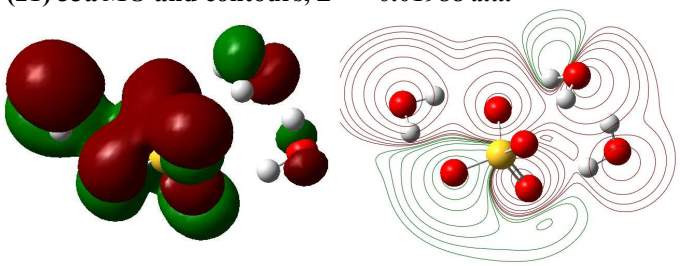

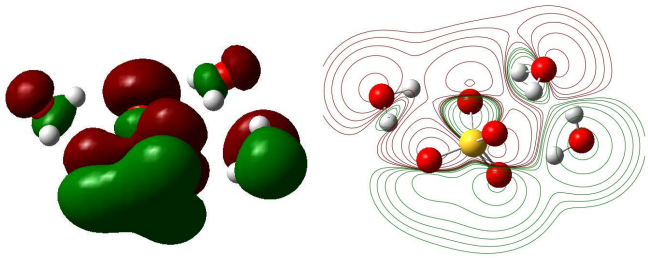

(22) 34a MO and contours, *E* = +0.02545 *a.u.*

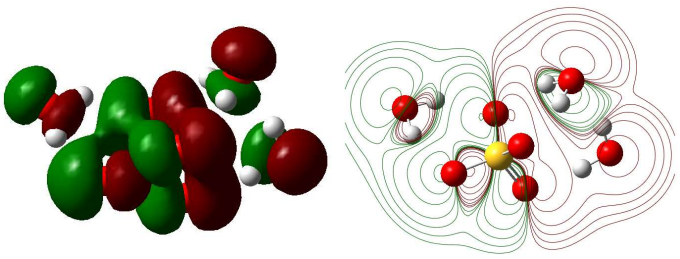

(23) 35a MO and contours, *E* = +0.02687 *a.u.*

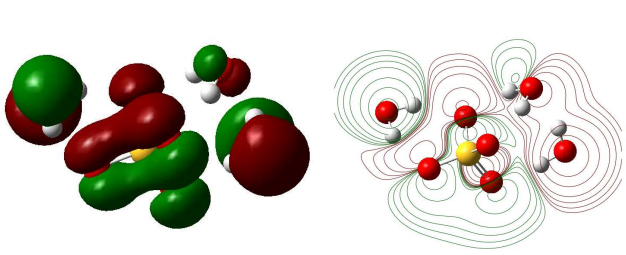

(24) 36a MO and contours, *E* = +0.02957 *a.u.*

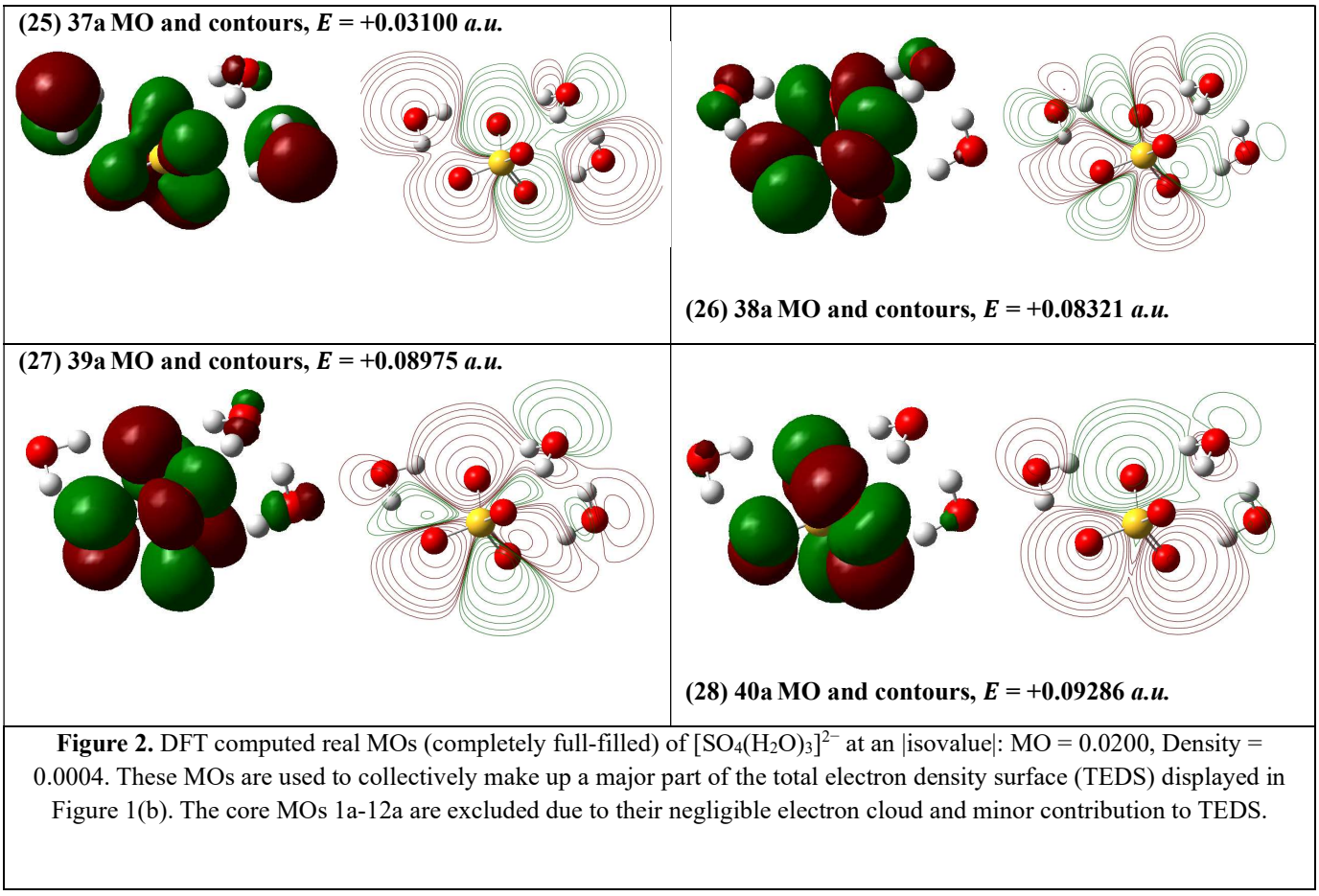

Figure 2. DFT computed real MOs (completely full-filled) of $[SO_4(H_2O)_3]^{2-}$ at an |isovalue|: MO = 0.0200, Density = 0.0004. These MOs are used to collectively make up a major part of the total electron density surface (TEDS) displayed in Figure 1(b). The core MOs 1a-12a are excluded due to their negligible electron cloud and minor contribution to TEDS.

3.1.2 Mulliken Population Analysis

Despite the potentialities of electron density surfaces (both total and individual) and their mapping techniques (contour diagrams) in revealing semiquantitative type information of the chemical bonding and specific electronic interactions (subsection **3.1.1**), the theoretically computed numerical values of the atomic charges are desperately needed for the purpose of quantifying and comparing specific type atomic interactions. In other words, the theoretical computing of the partial atomic charges and their assignment to each individual atom is always a foremost step for primary explanation of qualitative charge distribution in the entire molecular specimen and the approximation of wherein the electron density probably resides. In an attempt to derive numeral values of the atomic charges computationally, the population analysis method must be implemented through the *Gaussian* run *ab initio* based mathematical algorithms [24]. This method is actually used for analyzing the electron density in the molecular systems. When the computational procedure is on the fly, this method divides up the density $D_{\alpha\beta}$ and overlap matrix terms $S_{\alpha\beta}$ of the orbital occupation expression $\rho(r) = D_{\alpha\beta}S_{\alpha\beta}$, and determines numeral atomic charges mathematically. While over-interpretation of thus derived partial atomic charge distributions in the entire molecular specimen is not recommended due to their inability to describe any observable properties of the atoms or molecule itself, the Mulliken (wave function based population analysis method) derived numeral value of partial atomic charge of each atom is highly useful to understand atomic charge distribution and specific bonding interactions qualitatively. Additionally, the Mulliken derived atomic charges are quite useful in force field calculations (as an effective parameter) as well as in comparing chemical properties of the two closely related molecular systems [24]. The brief mathematical operations that are incorporated under Mulliken analysis are to sum up all the populations of all the concerned atomic orbitals on a single atom, and then subtract to nuclear charge, giving a resultant partial atomic charge on each atom. Even though an absolute magnitude of the partial atomic charges computed through Mulliken method displays a high degree of sensitivity to the types of basis set used, and therefore, is subjected to vary with respect to latter, the numeral values presented below are only restricted to the basis set of the type 6−31G (*d, p*) used in this study.

The DFT derived partial atomic charges on the Sulphur (S), Hydrogen (H), and Oxygen (O) atoms of the $[SO_4(H_2O)_3]^{2-}$ ion are presented in Table 1, where all the numerically labeled atoms are in accordance with the atomic label used in Figure 3. Based on the intensity of these numeral atomic charges, all the atoms are colored and displayed in the form of a low energy ground state electronic structure (Figure 3), where color index and range are clearly mentioned in inset. On the basis of this color index, it can be concluded that all the red colored (in central SO_4^{2-}: O2, O3, O4, and O5; in three surrounding H_2O: O6, O9, O12), the most green colored (in central SO_4^{2-}: S1), and the dark green colored (in three surrounding H_2O: H7, H8, H10, H11, H13, and H14) spheroids represent the most negatively, most positively, and comparatively least positively charged atoms respectively. This inhomogeneous partial atomic charges distribution in $[SO_4(H_2O)_3]^{2-}$ indicates that there is an asymmetric distribution of electrons in chemical bonds which is somewhat related to the electronic delocalization phenomenon occurred in the central SO_4^{2-} unit (this resonance is clearly seen in the central SO_4^{2-} unit of the DFT produced low energy ground state electronic structure of $[SO_4(H_2O)_3]^{2-}$ in Figure 2). The more quantitative aspects of these irregularities in partial atomic charges can be reconfirmed through their numeral values listed in Table 1. The most significant consequence caused by this asymmetric electronic distribution in $[SO_4(H_2O)_3]^{2-}$ is the origination of six hydrogen bonds in between partial negatively charged O atoms (O2, O3, O4, and O5) of the central SO_4^{2-} unit and more partial positively charged H atoms (H7, H8, H10, H11, H13, and H14) of the surrounding three H_2O molecules. Meanwhile, such inhomogeneous charge distributions are mostly arose due to a strong ability of the O atom to attract a bond pair towards itself as its electronegativity (χO = 3.44 in Pauling scale) is significantly greater than that for the S (χS = 2.58 in Pauling scale) and H (χH = 2.20 in Pauling scale) atoms. This electronegativity effect is intensely observed in the H−bonded O and H atoms as observed in both Figure 2 and Table 1. As a whole, the Mulliken derived partial atomic charges and their qualitative distribution throughout

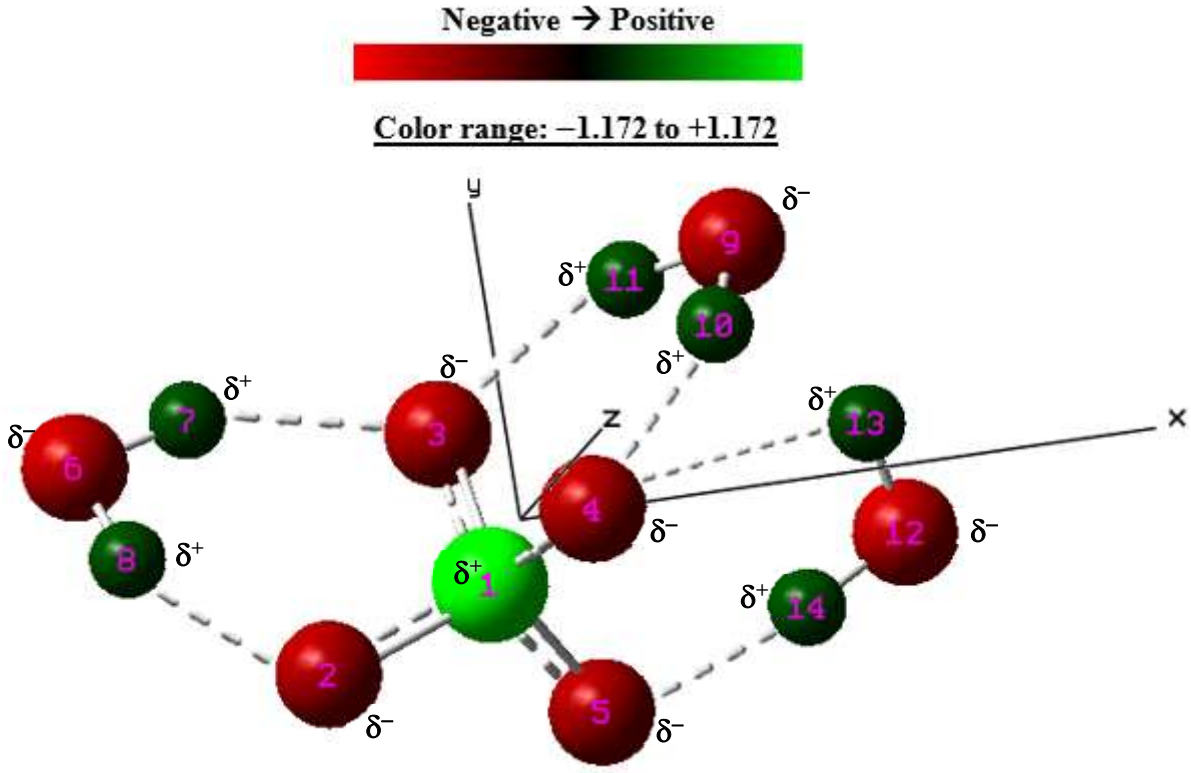

Figure 3. Mulliken charges distribution in the DFT optimized structure of $[SO_4(H_2O)_3]^{2-}$. All the atoms are labeled numerically and colored by intensity of atomic charges. The color range and index are shown in inset.

$[SO_4(H_2O)_3]^{2-}$ has indicated the occurrence of asymmetric type electronic distributions in all the chemical bonds, and the utmost irregularity of the electronic distribution observed in the chemical bonds between two more-electronegative and less-electronegative

atoms has marked them as polar bonds.

Table 1. Mulliken charges distribution in $[SO_4(H_2O)_3]^{2-}$ ion. The atoms are labeled in accordance with Figure 2.

S. No.	Atoms	DFT derived partial atomic charges (*a. u.*)
1	S1	+1.172
2	O2	− 0.691
3	O3	−0.731
4	O4	−0.702
5	O5	−0.675
6	O6	−0.757
7	H7	+0.310
8	H8	+0.310
9	O9	−0.717
10	H10	+0.317
11	H11	+0.318
12	O12	−0.765
13	H13	+0.284
14	H14	+0.327
Sum of Mulliken atomic charges = −2.00 *a.u.*		

IV. Conclusion

In this communication, the molecular orbitals based quantum mechanical views were expressed for confirming structural stability of the smallest yet stable microhydrated sulfate clusters $[SO_4(H_2O)_3]^{2-}$ (hydration number $n = 3$) existing predominantly in several sulfate enriched aqueous type chemical, biological, electrochemical, medicinal, and physiological systems. While acquiring the related quantum mechanical information, the wave function based fundamental methods such as molecular orbitals (MOs) and Mulliken population analyses were implemented computationally. Basically, these methods were used to extract DFT: B3LYP derived structural and chemical bonding information of $[SO_4(H_2O)_3]^{2-}$ from its molecular wavefunction (Ψ), to inquire quantitative picture of Ψthrough Ψ^2(total molecular electron density surface: TMEDS), and to examine all the iso-surfaces and contour lines of each occupied MO (except those for MOs). Due to being a well-formulated and a precisely modeled computational scheme designed mostly for incorporating even a minimal but a significant interactions of the micro-particles (in this case, SO_4^{2-} and H_2O), the DFT based quantum mechanical model became the first choice for this study without which an exact determination of low energy electronic structure and the quantitative estimation of the concerned 3D electron density surfaces couldn't be achieved properly.

The general results show that the TMEDS approximated the closed 3D molecular geometry of $[SO_4(H_2O)_3]^{2-}$ with symmetric and asymmetric electronic distributions around the specific atoms, and the clearly distinguishable protrusions projected on this surface depicted the most probable positions of three hydrogen-bonded H_2O molecules bound centrally to SO_4^{2-} unit in the

3D axis. Accordingly, all the electron density iso-surfaces assigned to each individual spin paired-MOs confirmed the electronic cloud delocalization phenomena occurred over the entire $[SO_4(H_2O)_3]^{2-}$ specimen which further not only approximated a region of space in which valence electrons are likely to be found but also assured the orbital type bonding interactions between two similar or dissimilar type atoms in MOs building up process. Beside this, the contour diagram for each MO exhibited the electron amplitudes quantitatively with a maximum departure of the electronic wave from average. In short, all the DFT derived electron density surface plots and the contour mappings of each occupied MO predicted a chemically bonded and an energetically stable structural entity of $[SO_4(H_2O)_3]^{2-}$ on the basis of molecular wave function based computations. In the support of the same, the Mulliken derived partial atomic charge on each atom of $[SO_4(H_2O)_3]^{2-}$ tentatively explained electronic redistribution throughout its structure which was indeed very much essential while quantifying and comparing specific type electronic interactions between any two bonding atoms.

REFERENCES

[1] M. Jung, W. Lee, C. Noh, A. Konovalova, G. S. Yi, S. Kim, Y. Kwon, D. Henkensmeier, *J. Memb. Sci.* **580**, 110(2019).

[2] D. Pavlov, *Lead Acid Batteries: Science and Technology* (Elsevier, 2011).

[3] Food and Nutrition Board, Institute of Medicine of the National Academies, *Dietary Reference Intakes for Water, Potassium, Sodium, Chloride, and Sulfate* (National academic press, 2005).

[4] Sodium Sulfate Functions in Daily Life–Formula–Uses, *https://azchemistry.com/sodium-sulfate-function.*

[5] D. Markovich, *Physiol. Rev.* **81**(4), 1499(2001).

[6] J. T. O'Brien, J. S. Prell, M. F. Bush, E. R. Williams, *J. Am. Chem. Soc.* **132**, 8248(2010).

[7] N. Hillebrandt, P. Vormittag, N. Bluthardt, A. Dietrich, J. Hubbuch, *Front. Bioeng. Biotech.* **8**, 489(2020).

[8] J. P. D. Abbatt, S. Benz, D. J. Cziczo, Z. Kanji, U. Lohmann, O. Möhler, *Science* **313**, 1770(2006).

[9] J. Flahaut, M. Massé, L. Le Deit, P.Thollot, J.-P. Bibring, F. Poulet, C. Quantin, N. Mangold, J. Michalski, J. L. Bishop, Sulfate-rich deposits on mars: a review of their occurrences and geochemical implications, Eighth International Conference on Mars (2014).

[10] X. Wang, J. B. Nicholas, L. Wang, *J. Chem. Phys.* **113**(24), 10837(2000).

[11] M. Kulichenko, N. Fedik, K. V. Bozhenko, A. I. Boldyrev, *J. Phys. Chem. B* **123**, 4065(2019).

[12] L. C. Smeeton, J. D. Farrell, M. T. Oakley, D. J. Wales, R. L. Johnston, *J. Chem. Theory Comput.* **11**, 2377(2015).

[13] A. T. Blades, P. Kebarle, *J. Phys. Chem. A* **109**, 8293(2005).

[14] A. B. Marahatta, *Int. J. Prog. Sc. Tech.* **25**(1), 595(2021).

[15] A. B. Marahatta, *Int. J. Prog. Sc. Tech.* **17**(1), 55(2019).

[16] A. B. Marahatta, *Int. J. Prog. Sc. Tech.* **27**(2), 441(2021).

[17] A. I. Boldyrev, J. Simons, *J. Phys. Chem.* **98**, 2298(1994).

[18] L. C. Smeeton, J. D. Farrell, M. T. Oakley, D. J. Wales, R. L. Johnston, *J. Chem. Th. Comput.* **115**, 2377(2015).

[19] A. T. Blades, P. Kebarle, *J. Am. Chem. Soc.* **116**, 10761(1994).

[20] P. Hunt, B. Kirchner, T. Welton, *Chem. Eur. J.* **12**(26), 6762(2006).

[21] F. Jensen, *Introduction to Computational Chemistry* (John Wiley & Sons, Chichester, 2003).

[22] W. L. Jolly, *Modern Inorganic Chemistry* (McGraw-Hill Book Company, New York, 1984).

[23] K. Fukui, *Science* **218**(4574), 747(1982).

[24] J. B. Foresman, Æ Frisch, *Exploring Chemistry with Electronic Structure Methods* (Gaussian, Inc.: Wallingford, CT, 2015).

[25] R. S. Mulliken, *J. Chem. Phys.* **23**, 1833(1955).

[26] M. D. Segall, R. Shah, C. J. Pickard, M. C. Payne, *Phys. Rev. B* **54**(23), 16317(1996).

[27] P. Hohenberg, W. Kohn, *Phys. Rev. B* **136**(3B**)**, 864(1964).

[28] W. Kohn, L. Sham, *Phys. Rev. J.* **140**(4A**)**, A1133(1965).

[29] A. B. Marahatta, *Int. J. Prog. Sc. Tech.* **16**(1), 51(2019).

[30] A. B. Marahatta, *Int. J. Prog. Sc. Tech.* **16**(2), 01(2019).

[31] B. Wang, S. L. Li, D. G. Truhlar, *J. Chem. Theory Comput*. **10**, 5640(2014).

[32] A. B. Marahatta, *Int. J. Prog. Sc. Tech.* **23**(2), 541(2020).

[33] Æ. Frisch, H. P. Hratchian, R. D. Dennington II, T. A. Keith, J. Millam, *Gauss view 05 Reference* (Gaussian, Inc.: Wallingford, CT, 2009).

[34] Gaussian 09 manual. *http://gaussian.com/geom/?tabid=1#GeomkeywordReadOptimi zeoption*

[35] Æ. Frisch, *Gaussian 09W Reference* (Gaussian, Inc.: Wallingford, CT, 2009).

[36] J. Rigby, E. I. Izgorodina, *Phys. Chem. Chem. Phys.* **15**, 1632(2013).

[37] G. V. Gibbs, A. F. Wallace, D. F. Cox, R. Downs, N. L. Ross, K. M. Rosso, *Am. Mineral.* **94**, 1085(2009).

[38] L. Pauling, *J. Chem. Educ*. **69**, 519(1992).

[39] G. Frenking, A. Krapp, *J. Comput. Chem.* **28**, 15(2007).

[40] M. Fugel, J. Beckmann, D. Jayatilaka, G. V. Gibbs, S. Grabowsky, *Chem. Eur. J.* **24**, 6248(2018).

[41] J. D. Lee, *Concise Inorganic Chemistry For JEE (Main & Advanced)*, 4th ed. (Wiley India, 2018).